BIOCHEMISTRY
including biophysical chemistry & molecular biology

Article

pubs.acs.org/biochemistry

Structural Effects and Lipid Membrane Interactions of the pH-Responsive GALA Peptide with Fatty Acid Acylation

Brian F. Lin,[†,‡,§] Dimitris Missirlis,[*,†,§,§] Daniel V. Krogstad,[∥] and Matthew Tirrell[†,∥,⊥]

[†]Department of Bioengineering, University of California, Berkeley, California 94720, United States
[‡]Department of Chemistry and Biochemistry, University of California, Santa Barbara, California 93106, United States
[§]Department of Biophysical Chemistry, Institute for Physical Chemistry, University of Heidelberg, Heidelberg, D-69210, Germany
[∥]Materials Department, University of California, Santa Barbara, California 93106, United States
[⊥]Institute for Molecular Engineering, University of Chicago, Chicago, Illinois 60637, United States

Supporting Information

ABSTRACT: GALA is a pH-responsive, membrane-perturbing peptide designed to fold from a random coil at physiological pH to an amphipathic α-helix under mildly acidic conditions. Because of its pH-activated function, GALA has been sought-after as a component of intracellular drug delivery systems that could actively propel endosomal escape. In this study, we conjugated GALA with lauryl and palmitoyl fatty acid tails as model hydrophobic moieties and examined the physicochemical characteristics and activities of the resulting peptide amphiphiles (PAs). The fatty acid variants of GALA exhibited distinctly different membrane perturbing mechanisms at pH 7.5 and 5.5. At physiological pH, the PAs ruptured liposomes through a surfactant-like mechanism. At pH 5.5, lauryl-GALA was shown to form transmembrane pores with a higher potency as compared to its unmodified peptide counterpart; however, after prolonged exposure it also caused liposome lysis. The lytic activity of fatty acid-conjugated GALA did not impair cell viability. Lauryl-GALA was tolerated well by SJSA-1 osteocarcinoma cells and enhanced cell internalization of the PA was observed. Our findings are discussed with the overarching goal of developing efficient therapeutic delivery systems.

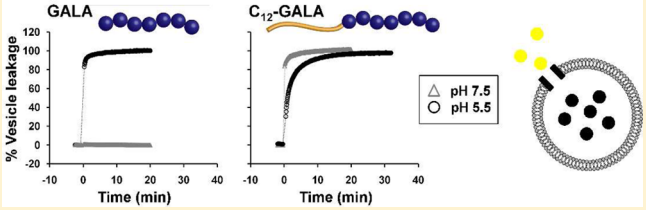

Natural organisms and viruses utilize stimuli-responsive, membrane-perturbing peptides for a variety of functions including membrane fusion and self-defense in the form of toxins and antimicrobials.[1,2] A major subset of these peptides has adopted amphipathic α-helices as their functional form.[1] While in solution these peptides are mostly random coils. Stimuli such as pH changes or interactions with membrane lipids and ligands induce folding into the functional conformation. Despite their small size, these peptides are capable of cooperatively perturbing biological membranes through mechanisms such as membrane thinning and pore formation.[3] The selectivity and efficacy of these peptides have resulted in numerous efforts toward employing them as components in drug delivery systems[4] and at the same time have inspired the design of synthetic analogues.[5−7]

One example of such a biomimetic analogue is the pH-responsive, fusogenic peptide GALA, designed by Szoka et al.[8] GALA is a 30 amino acid peptide (WEAALAEALAEALAEH-LAEALAEALEALAA) that transitions from a mostly random coil conformation at physiological pH to an amphipathic α-helix as pH is lowered below 6.[9] GALA helices are then capable of binding lipid membranes and, at a sufficiently high surface concentration, self-associate to form transmembrane pores. Approximately 10 peptides are required to form a stable pore, which allows diffusion of small molecules across the bilayer.[10] These characteristics make GALA a promising candidate for enhancing small molecule transport through lipid membranes in situations where pH is reduced. For example, when drug delivery systems are internalized via receptor-mediated endocytosis, acidification of endosomes occurs as they are trafficked from the plasma membrane toward lysosomes. This pH reduction would trigger GALA activity and enhance escape of endosomal contents into the cytoplasm.[11−15]

A challenge for the *in vivo* use of GALA is its practical incorporation into a drug delivery system.[15] *In vitro* cell studies employing unmodified GALA in presence of a drug delivery system cannot be translated to a clinical setting because the peptide lacks targeting abilities and therefore is ineffective *in vivo*. Fusion of GALA to therapeutic and/or targeting sequences would pose difficulties in synthesis and handling due to the increased peptide length. One attractive alternative is to incorporate the peptide into multifunctional, self-assembled nanoparticles such as liposomes or micelles. This can be achieved by modifying GALA with a hydrophobic anchor, such as a fatty acid or a lipid.[16,17] Under these circumstances the fate of the peptide is coupled to that of the nanoparticle, which can

Received: March 5, 2012
Revised: May 15, 2012
Published: May 16, 2012

   dx.doi.org/10.1021/bi300314h | *Biochemistry* 2012, 51, 4658−4668

then be tailored with targeting moieties and therapeutic agents.[18] A similar strategy has been previously examined, where GALA was conjugated to cholesterol and integrated into transferrin-decorated liposomes.[14] GALA-tethered liposomes showed improved efficiency for delivering fluorescent probes as compared to the use of encapsulated GALA or GALA that was free in solution *in vitro*. The liposomes were further employed to enhance nucleic acid transfection in cultured cells.[14,19,20] In another study, fatty acid modification was employed for a shorter version of GALA termed short fusogenic peptide.[21] The authors observed a 1000-fold enhancement in membrane-destabilizing power for the myristoylated peptide derivative. Despite the increase in activity conferred through such modifications of GALA, their effects on peptide structure and interactions with model membranes have not been addressed in detail. In this work, we modified GALA with two different fatty acid tails as the hydrophobic moiety and examined its membrane associating mechanism in an attempt to optimize GALA effectiveness.

A direct effect of peptide acylation is that PAs self-assemble into micelles above a critical micelle concentration (CMC). The CMC depends on the length and hence the hydrophobicity of the alkyl chain.[22,23] Above the CMC, dynamic equilibrium between micelles and isolated monomers in solution is established. Self-assembly of PAs in solution was suggested previously, to play a crucial role on peptide activity.[24−26] For example, modification of a cationic amphipathic peptide termed AKK showed an increase in activity with increasing chain lengths up to 16 carbons. For longer tails, activity was reduced, presumably due to the formation of micelles that reduced the effective monomer concentration.[24]

On the micelle surface, bioactive peptides are presented in a high density, and as a consequence of peptide crowding, secondary structure is induced. This was previously shown for a number of peptides varying in length, secondary structure, and functionality,[27−31] including antimicrobial and synthetic fusogenic peptides, which share structural and functional similarities to GALA.[24−26,29,32,33] In most cases, bactericidal activity of PAs was increased as compared to the parent peptides. This observation was attributed to the enhancement of both helical stability and membrane affinity.

In this study, we report on how GALA modified with either lauric or palmitic acid affects peptide folding and membrane perturbing activity. Our results shed light onto the effects of peptide acylation and provide some fundamental insight into the use of GALA PAs, as well as that of similar peptides, for therapeutic applications. Additionally, we investigated how GALA acylation affected cell interactions *in vitro* as a preliminary step toward their biofunctional characterization. Our findings are discussed having in mind the overarching goal of constructing efficient drug delivery systems.

EXPERIMENTAL PROCEDURES

Materials. GALA peptide (WEAALAEALAEALAEHLAEALAEALEALAA) capped with an N-terminal fluorenylmethyloxycarbonyl (Fmoc) group and protected amino acid side chains on a Wang resin was purchased from Suzhou ChinaTech Peptide Co. Egg phosphatidylcholine (PC) was purchased from Avanti Polar Lipids. Lauric acid, palmitic acid, calcein, fluorescein isothiocyanate-dextran (FitC-Dextran; MW 4000), trifluoroacetic acid (TFA), *N,N*-diisopropylethylamine, ammonium thiocyanate, ferric chloride hexahydrate, dimethylformamide, acetonitrile, chloroform, tetrahydrofuran, triisopropylsilane, triton X-100, sephadex G-25, sodium hydroxide, and hydrochloric acid were purchased from Sigma-Aldrich. Monosodium phosphate monohydrate, disodium phosphate heptahydrate, and 50 kDa dialysis tube were purchased from Fisher Scientific. Fmoc-6-aminohexanoic acid and *N*-α-Fmoc-*N*-ε-1-(4,4-dimethyl-2,6-dioxocyclohex-1-ylidene)ethyl-L-lysine (Fmoc-lysine(Dde)-OH) were purchased from Novabiochem. *N*-Hydroxybenzotriazole monohydrate (HOBt) was purchased from Advanced ChemTech. 2-(1*H*-benzotriazole-1-yl)-1,1,3,3-tetramethyluronium hexafluorophosphate (HBTU) was purchased from Advanced Automated Peptide Protein Technologies. 3-(4,5-Dimethylthiazol-2-yl)-2,5-diphenyltetrazolium) bromide (MTT) was purchased from Invitrogen. 5(6)-Carboxytetramethylrhodamine and pyrene were purchased from Fluka. SJSA-1 cell line, RPMI 1640 cell media, and GIBCO calf bovine serum (CBS) were purchased from American Type Culture Collection (ATCC). GIBCO penicillin−streptomycin and hoechst 33342 dye were purchased from Invitrogen. Pyrene was recrystallized from ethanol prior to use.

Peptide and PA Preparation. Peptide modifications were performed on the resin, adapting solid phase synthesis methods previously described.[34] Orthogonally protected, hydrazine-cleavable Fmoc-lysine(Dde)-OH was used for the conjugation of fluorophores. Fmoc-6-aminohexanoic acid was employed to space fluorophores from peptides. Peptides and PAs were cleaved from the resin with a standard TFA cleavage solution, precipitated in diethyl ether, and purified on a Shidmadzu CBM-20A high performance liquid chromatography (HPLC) system, in reverse phase, employing a Waters Symmetry 300 semipreparative C4 column. Product identity was confirmed by mass spectrometry employing an Applied Biosystems 4700 Proteomics Analyzer, and purity was determined using analytical HPLC with a Waters Symmetry 300 analytical column. All peptides and PAs employed in this study had purities above 90%. Their molecular structures are given in the Supporting Information (Figure S1).

Buffers. Stock solutions of phosphate buffer (PB) and phosphate buffer containing potassium chloride (PB/KCl) were prepared with Milli-Q quality water at 10× the working concentration (100 mM of phosphate and 1 M KCl for PB/KCl stock). Buffers were adjusted to pH 7.5 ± 0.1 or 5.5 ± 0.1 with a minimal amount of either concentrated HCl or NaOH.

Liposome Preparation. Liposomes composed of egg PC were prepared using the film hydration method.[35] Briefly, a dried film of egg PC on glass was hydrated in buffer for 1 h at 70 °C to produce multilamellar vesicles. This was then followed by three freeze−thaw cycles and 10 extrusions through a 100 nm nominal pore sized polycarbonate filter (Millipore) in a temperature-controlled extruder, set at 37 °C. Liposomes that encapsulated calcein or FITC-dextran (4000 MW) were prepared by hydrating films with corresponding solutions. Nonencapsulated material was removed with a Sephadex G-25 size exclusion column followed by dialysis with 50 kDa MW cutoff membrane tubes.

The concentration of egg PC was quantified using a previously described colorimetric method.[36] Briefly, 100 μL of egg PC solution was added to 1 mL of ammonium ferrothiocyanate (100 mM) and 2 mL of chloroform, and then the mixture was vigorously mixed. The chloroform phase was then extracted, and its absorbance at 488 nm was measured on

Table 1. Peptides and PAs Used in This Study

abbreviation	sequence[a]	theor mass	measd mass [M + Na]
GALA	WEAALAEALAEALAEHLAEALAEALEALAA	3030.55	3052.10
Rho-GALA	K(Rho)X-GALA	3555.78	3580.49
C_{12}-GALA	lauryl-GALA	3212.72	3234.61
C_{12}-Rho-GALA	lauryl-K(Rho)X-GALA	3866.04	3885.30
C_{16}-GALA	palmitoyl-GALA	3268.72	3291.10

[a]One-letter code for amino acids. W: tryptophan; E: glutamic acid; A: alanine; L: leucine; H: histidine; K: lysine. Additional abbreviations: X: 6-hexaminoic acid; C_{12}: lauryl; C_{16}: palmitoyl; Rho: tetramethylrhodamine.

a Shidmadzu UV-3600 spectrometer. Concentration was determined using a standard curve.

Critical Micelle Concentration (CMC) Determination. CMC was determined using the pyrene solubilization method.[37] PAs at varying concentrations were dissolved in an aqueous pyrene stock solution (1×10^{-6} M) containing traces of tetrahydrofuran and left to equilibrate at 37 °C for 1 h. Emission intensities at 373 nm (P_1) and 393 nm (P_3) were recorded at varying PA concentrations using a TECAN Infinite M200 instrument in 96-well plates, and the intensity ratio of the third (P_3) to the first (P_1) vibrational band of pyrene was calculated. CMC was determined as the onset of P_3/P_1 increase.

Circular Dichroism (CD) Spectroscopy. Peptide folding was studied by ultraviolet CD spectroscopy on a Jasco J-815 spectropolarimeter with temperature control. CD spectra in the range of 250 to 190 nm were acquired using cuvettes with either 1 or 10 mm path length. Reported spectra are averages of three individual scans.

Liposome Leakage Assay. Membrane disruption was probed using liposome leakage assays that monitored the release of encapsulated calcein (150 mM) from liposomes. 100 μL of liposome suspensions (100 μM) was mixed with 1 μL of peptide or PA solutions at varying peptide-to-lipid (P:L) ratios. The solutions were incubated for 120 min at room temperature. Then their fluorescence emission intensity at 490 nm, excited at 395 nm, was measured using a TECAN Infinite M200 instrument. Calcein release was calculated using the equation

$$\% \text{ leakage} = \frac{I - I_0}{I_{max} - I_0} \quad (1)$$

I, I_0, and I_{max} are the calcein fluorescence intensity after 120 min, the background intensity, and the maximum intensity corresponding to complete leakage induced by Triton X-100, respectively. Leakage values are averages of three individual experiments.

Leakage kinetic curves were obtained using a Jasco FP 6500 fluorescence spectrometer. 100 μL of liposome suspensions (100 μM) was placed in a quartz cuvette and equilibrated at room temperature for 1 h. Fluorescence intensity was then recorded every 5 s. After ∼2 min, 1 μL of peptide or PA solution was added to the liposomes and mixed thoroughly by pipetting.

Dynamic Light Scattering (DLS). DLS was performed on a Brookhaven Instruments system that consisted of an avalanche photodiode detector, which measured scattering intensity from a suspension illuminated by a Melles Griot 632.8 nm HeNe laser as a function of delay time. Temperature was maintained at 25.0 ± 0.1 °C using a circulating water bath. The first-order autocorrelation function was measured at 90° (q = 0.0189 nm^{-1}). The autocorrelation function was then fit using a second-order cumulant to extract the average decay rate, Γ_1. The quantity Γ_1/q^2 was then taken as the apparent diffusion coefficient, D_{app}, and the hydrodynamic diameters were calculated using the Stokes−Einstein equation. Scattering intensity was measured as events per second (counts/s) at 90°.

Cryogenic Transmission Electron Microscopy (Cryo-TEM). Samples for cryogenic imaging were prepared at a total organic concentration of 300 μM. GALA peptides or PAs were incubated with egg PC liposomes for 10 min at a P:L ratio of 1:100. Then 3.5 μL of the mixture was transferred onto a glow discharged lacey carbon-coated copper grid. The samples were vitrified using an environmentally controlled FEI Vitrobot Mark IV with the temperature set at 24 °C and humidity at 100%. Samples were placed in a Gatan cryo-holder and kept below −170 °C throughout imaging. Imaging was performed at 200 kV using the low dose mode with an FEI Technai G2 Sphera microscope. Cryogenic images were recorded digitally with a Gatan Ultrascan 1000 CCD camera and analyzed using the Gatan Digital Micrograph software.

***In Vitro* Cell Experiments.** The human osteosarcoma SJSA-1 cell line was cultured to exponential growth, subconfluent monolayers in RPMI-1640 culture medium, supplemented with 10% v/v calf bovine serum, and 1% v/v penicillin−streptomycin. Cells were grown at 37 °C in a humidified atmosphere with 5% CO_2. SJSA-1 cells were seeded at a density of 15×10^3 cells/cm^2 and were allowed to attach on surfaces for 12 h. Cell proliferation was measured using a MTT assay. Briefly, after 24 h incubation with Rho-GALA or C_{12}-Rho-GALA, cells were washed twice with PBS and then supplemented cell culture medium containing 0.5 mg/mL MTT was added. After 3 h, the medium was removed and 100 μL of methanol and dimethyl sulfoxide at a ratio of 1:1 was added. The extent of MTT reduction was measured through absorbance at 595 nm. Results are reported as percent proliferation relative to control cells, which received no treatment.

Internalization of Rho-GALA or C_{12}-Rho-GALA was assessed using a Zeiss LSM 700 laser scanning confocal microscope. Briefly, SJSA-1 cells were incubated with Rho-GALA or C_{12}-Rho-GALA at a concentration of 25 μM for 1 h in supplemented cell culture medium. Hoechst 33342 was added and incubated for 10 min to stain cell nuclei. Finally, the cells were washed three times with cold PBS and imaged in supplemented cell culture medium. Alternatively, cells were fixed with 4% paraformaldehyde in 100 mM phosphate buffer for 30 min, washed twice with PBS, and imaged.

RESULTS

Peptide and PAs. The pH-responsive, fusogenic GALA peptide was modified with two different fatty acid tails, and fluorescently labeled analogues were prepared with rhodamine tags (Table 1). A lauryl or a palmitoyl tail was conjugated via an amide bond to the N-terminus of GALA, resulting in PAs C_{12}-GALA and C_{16}-GALA, respectively. Rho-GALA and C_{12}-Rho-

dx.doi.org/10.1021/bi300314h | Biochemistry 2012, 51, 4658−4668

GALA were synthesized by conjugating rhodamine on the ε-amine of an orthogonally protected lysine introduced at the peptide N-terminus. Rhodamine-labeled lysines were spaced from the peptide using 6-aminohexanoic acid in order to avoid hindering the activity of GALA. The chemical structures of the peptides and PAs are provided in the Supporting Information (Figure S1). The CMC of GALA PAs decreased as the fatty acid tail length increased from 12 to 16 carbons (Table 2 and Figure S2). Self-assembly was dependent on solution pH: at pH 5.5, the CMC of both PAs was effectively lowered due to protonation of glutamate side chains.

Table 2. CMC (in μM) of PAs at pH 5.5 and 7.5 in PB/KCl Buffer

PA	pH 5.5	pH 7.5
C_{12}-GALA	7	29
C_{16}-GALA	1	3

GALA Secondary Structure. CD spectroscopy was employed to monitor the secondary structure of GALA peptides and PAs in response to pH and ionic strength. Spectra were acquired with 50 μM of analyte, which corresponds to PA concentrations above their CMC. All CD spectra exhibited an isosbestic point at 203 nm, which indicated that GALA transitioned exclusively between random coil and α-helical states.

CD spectra of the peptide confirmed previous results, showing a shift from a mostly random coil conformation at pH 7.5 to an α-helix at pH 5.5 (Figure 1A). In contrast, GALA PAs exhibited high helical contents at physiological pH, with C_{16}-GALA having higher helical content as compared to C_{12}-GALA in PB. At pH 5.5, both PAs were completely helical (Figure 1B). Increasing ionic strength via addition of 100 mM KCl enhanced peptide folding. This enhancement in presence of salt is attributed to the charge screening between glutamate side chains and is consistent with previous studies.[9]

At pH 5.5, the peptide and both PAs exhibited a similar degree of helicity. In order to distinguish differences in their helical stability, we monitored ellipticity changes at 222 nm as a function of temperature (Figure 2). GALA peptide unfolded rapidly above 60 °C, whereas both PAs exhibited a lower degree of unfolding, which was more gradual. This result indicated that helices on the micelle surface were more stable than those of the unmodified peptide. Heating and cooling curves overlapped suggesting that folding was reversible.

The secondary structure stabilization in PA micelles is thought to originate from the loss of peptide conformational freedom upon self-assembly, which counterbalances the entropic cost of folding.[27] Therefore, if PA concentration would drop below the CMC, no secondary structure enhancements would be observed. Indeed, as observed in Figure 3, helicity of GALA PAs decreased with decreasing concentration and below the CMC their helical content approached that of the peptide.

Overall, our CD results revealed that acylation of GALA peptide enhanced its α-helical folding above the CMC of the PAs, at all pH and ionic strengths studied.

Liposome Leakage Assay. GALA activity was monitored using a leakage assay with small unilamellar egg PC liposomes that contained calcein above its self-quenching concentration. In the event of membrane disruption or pore formation, calcein would escape from the liposome to the aqueous surrounding. Consequently, calcein would be diluted and the fluorescence intensity of the solution would increase. The extent of calcein leakage at equilibrium was determined using eq 1.

Initially, GALA peptide-induced leakage of calcein was measured. Consistent with previous reports,[9] the peptide did not induce significant leakage at pH 7.5, whereas at pH 5.5 liposome leakage was proportional to the peptide concentration (Figure 4). The dependence of leakage extent as a function of peptide-to-lipid (P:L) ratio matched previously reported values.[10] This validated our experimental setup, which we further employed to examine membrane disruption by PAs.

PAs induced the leakage of calcein at both pH values examined, (Figure 4). At pH 7.5, leakage was observed from P:L ratios of 1:10000 and 1:100000 for C_{12}-GALA and C_{16}-GALA, respectively. The fact that PAs disrupted liposomes at physiological pH suggested that acylation resulted in a fundamentally different mechanism of leakage as compared to the unmodified peptide.

At pH 5.5, a lower amount of C_{12}-GALA was required to induce calcein leakage relative to unmodified GALA or C_{16}-GALA (Figure 4). One possible explanation for the increase in potency of C_{12}-GALA over the peptide is that its increased hydrophobicity enhances liposome association and thus lowers the effective PA concentration for leakage. This result is consistent with a trend previously described with an analogous pH responsive fusogenic peptide.[21] However, the same reasoning would predict even higher activity for C_{16}-GALA since it is the most hydrophobic counterpart in this study. Therefore, tail hydrophobicity and membrane association are not the only determinants for activity.

We next examined whether PA micellization inhibited leakage activity. Measurements with C_{16}-GALA at 10 times lower lipid concentrations were performed, so that PA concentrations were well below their CMC (Figure S3). Leakage was slightly more effective at the higher lipid concentrations, indicating that micelle formation did not impair activity.

In order to gain better insight into the mechanism of action, we performed kinetics measurements of calcein leakage from liposomes incubated with either GALA or C_{12}-GALA. At pH 7.5, GALA did not release calcein, while at pH 5.5 the leakage kinetics was similar to previously reported data (Figure 5).[10] In contrast, C_{12}-GALA induced rapid leakage of calcein at P:L ratios of 1:100 and 3:1000, at pH 7.5. At pH 5.5, leakage kinetics was slower compared to pH 7.5. Moreover, C_{12}-GALA acted slower than GALA despite its higher potency at equilibrium leakage experiments. This observation suggested that either a different mechanism was responsible for leakage or that the process of pore formation was significantly delayed as a result of the acyl modification.

Thus far, our experimental data showed that PAs caused rapid and extensive leakage at pH 7.5 but did not elucidate the membrane perturbing mechanism. It was shown previously that GALA peptides assembled into pores that allow size-dependent diffusion of small molecules of 800 MW or less.[10] In order to determine whether PAs caused leakage by forming stable pores similar to the peptides, we encapsulated FITC-dextran (4000 MW), a high MW solute, and monitored its leakage following the addition of either GALA or C_{12}-GALA. If C_{12}-GALA were to form pores in the same manner as the peptide, no leakage of dextran would be observed. In contrast, rupturing liposomes via a surfactant-like mechanism (i.e., breaking up the lipid bilayer) would result in the release of the high MW molecules. As

dx.doi.org/10.1021/bi300314h | Biochemistry 2012, 51, 4658−4668

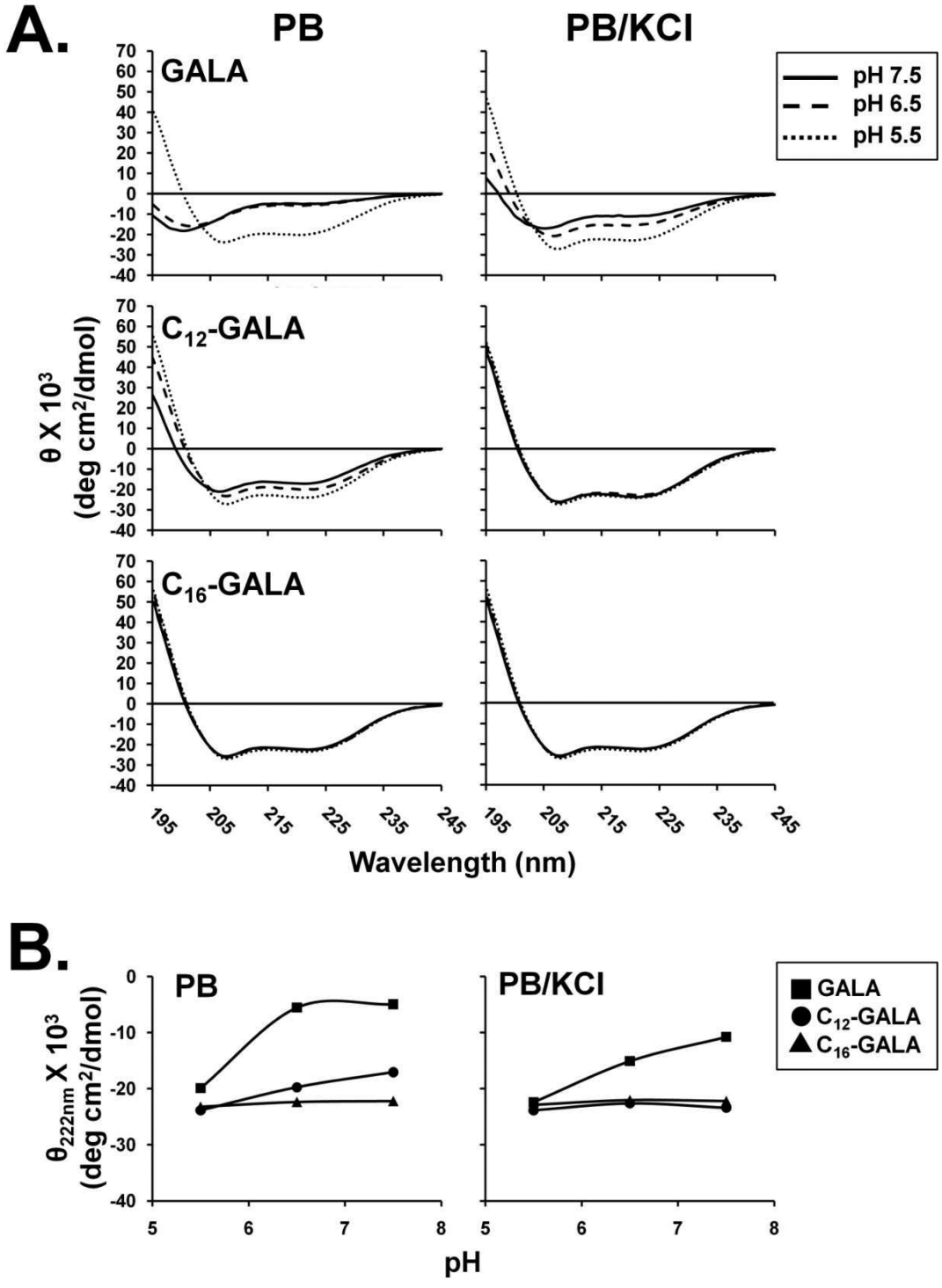

Figure 1. Increasing pH and ionic strength and GALA acylation led to enhanced peptide folding. (A) Circular dichroism spectra of GALA, C_{12}-GALA, and C_{16}-GALA at different pH values in PB buffer (left column) and PB/KCl buffer (right column). (B) Molar ellipticity at 222 nm as a function of pH for GALA, C_{12}-GALA, and C_{16}-GALA in PB (left) and PB/KCl (right).

expected, within 1 h incubation, GALA induced no leakage of dextran at either pH (Figure S4). C_{12}-GALA, on the other hand, induced dextran leakage at both pH values studied, albeit with markedly different kinetics. At pH 7.5, liposome rupture was complete within 5 min at a P:L ratio of 1:10 and at a P:L ratio of 1:100 leakage was above 90%. At the lower pH however, FITC-dextran leakage was dependent on the P:L ratio. At P:L of 1:10 virtually complete leakage was recorded at 5 min, whereas at 1:100 P:L ratio signs of leakage were detected only after an hour. These results suggest that the addition of a fatty acid tail on GALA induced liposome rupture through a surfactant-like process that was kinetically driven and pH dependent. An alternative explanation would be that PAs, due to peptide modification, formed pores with sizes larger relative to those formed by GALA.[38] In order to investigate this scenario, we performed light scattering and cryo-TEM on liposomes incubated with either peptides or PAs.

dx.doi.org/10.1021/bi300314h | *Biochemistry* 2012, 51, 4658−4668

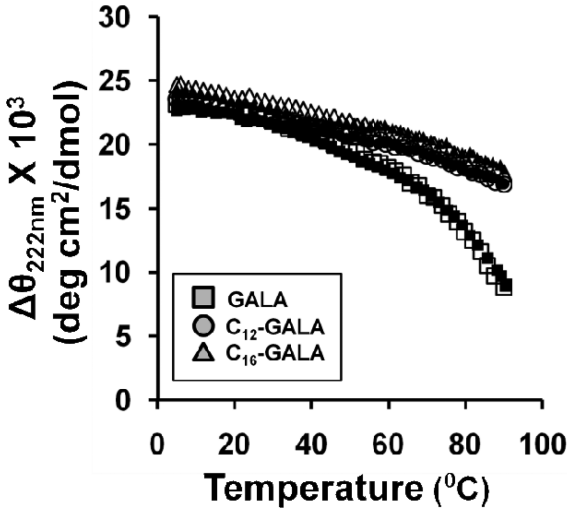

Figure 2. GALA α-helices are stabilized in PA micelles. Helix melting curves at pH 5.5, for GALA, C_{12}-GALA, and C_{16}-GALA in PB/KCl buffer. Both heating (solid symbols) and cooling ramps (open symbols) are presented.

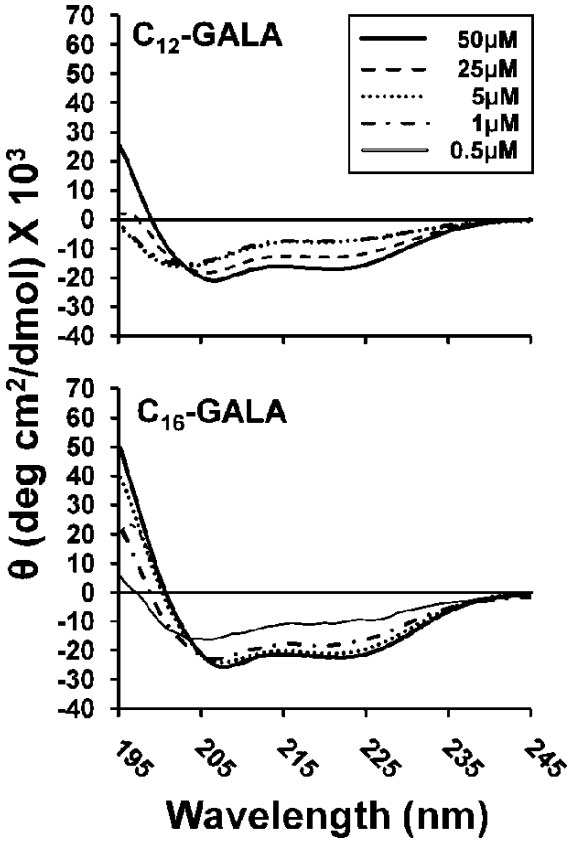

Figure 3. Secondary structure is stabilized through self-assembly. CD spectra of C_{12}-GALA (top) and C_{16}-GALA (bottom) at different concentrations in PB buffer at pH 7.5. The CMCs of the PAs are 29 μM for C_{12}-GALA and 3 μM for C_{16}-GALA.

Liposome Leakage Studied by Light Scattering and Cryo-TEM. Light scattering intensity, a function of particle size, was used to monitor liposome stability in the presence of either GALA or C_{12}-GALA. Initial experiments were performed at physiological pH and at P:L ratios of 1:10 and 1:100. GALA did not induce any noticeable changes to the liposome scattering intensity or size at the highest P:L ratio studied (Table 3). When C_{12}-GALA was simply added to the liposome suspension at a P:L ratio of 1:100, scattering intensity dips with subsequent rapid recoveries were recorded (Figure 6A). After mixing, the intensity plummeted and stabilized at a low value indicating the rupture of liposomes. The initial dips in the scattering intensity were most likely caused by bursting of liposomes in the detection volume, which only represented a miniscule fraction of the liposome suspension. Accordingly, mixing of the suspension allowed PAs to interact with the whole liposome population, causing their rupture and an irreversible minimization of the scattering intensity. At a P:L ratio higher by an order of magnitude, the effects were amplified. A rapid and complete loss of scattering intensity occurred immediately after the addition of PAs, even without mixing (Figure 6B).

At pH 5.5, light scattering results were markedly different. Exposure of liposomes to C_{12}-GALA at a 1:100 P:L ratio did not alter the scattering intensity after a 10 min (Figure 6A) or 1 h incubation (data not shown). At a 1:10 P:L ratio, addition of PAs slightly increased the scattering intensity by ~10%. After 30 min, the liposomes were larger in size (Table 3). The larger size and higher scattering intensity could reflect adsorption and/or pore formation of the PAs on the surface of the liposomes, causing bilayer extension. The observed increase in liposome diameter after GALA exposure, confirmed this scenario (Table 3).

Cryo-TEM was used to visualize liposome integrity upon exposure to GALA or C_{12}-GALA (Figure S5). At physiological pH, no liposomes were found after exposure for 10 min to C_{12}-GALA at a 1:10 P:L ratio. At pH 5.5, otherwise under the same conditions, liposomes were abundant when incubated with either GALA or C_{12}-GALA (Figure S5). This observation, in conjunction with the calcein and dextran leakage studies, suggests that short incubations with C_{12}-GALA induce the formation of transmembrane pores which only allow small materials to escape; however, with longer exposures the PA perturbs liposomes catastrophically, causing the release of contents independently of size.

Cytotoxicity and Cell Association. The liposome leakage results raised concerns regarding the use of GALA PAs in biological applications due to their potentially detrimental interaction with cell membranes at physiological pH. In order to examine cytotoxicity, Rho-GALA and C_{12}-Rho-GALA were incubated with SJSA-1 osteosarcoma cells for 24 h, and cell proliferation was measured using the MTT assay (Figure S6). Cell viability was not compromised when incubated with either 1000 μM Rho-GALA or 500 μM C_{12}-Rho-GALA. These were the highest concentrations studied in either case.

Having verified the cytocompatibility of Rho-GALA and C_{12}-Rho-GALA, we turned our attention to the mechanism of their interaction with cells, *in vitro*. The amphiphilic nature of PAs would presumably increase their cell association via nonspecific interactions between the fatty-acid tails and plasma membranes.[39,40] SJSA-1 osteosarcoma cells were incubated with 25 μM of rhodamine-labeled peptides or PAs and then visualized with laser scanning confocal microscopy using the same microscope settings (Figure 7). Qualitatively, C_{12}-Rho-GALA was internalized to a higher degree as compared to Rho-GALA. When live cells were imaged, uptake appeared to proceed via an endocytic pathway as peptides and PAs appeared to be localized in intracellular vesicles. It is important to note that fluorescence distribution was altered with cell fixation, causing it to appear diffuse (Figure S7). This is presumably due to the disruption of

dx.doi.org/10.1021/bi300314h | *Biochemistry* 2012, 51, 4658−4668

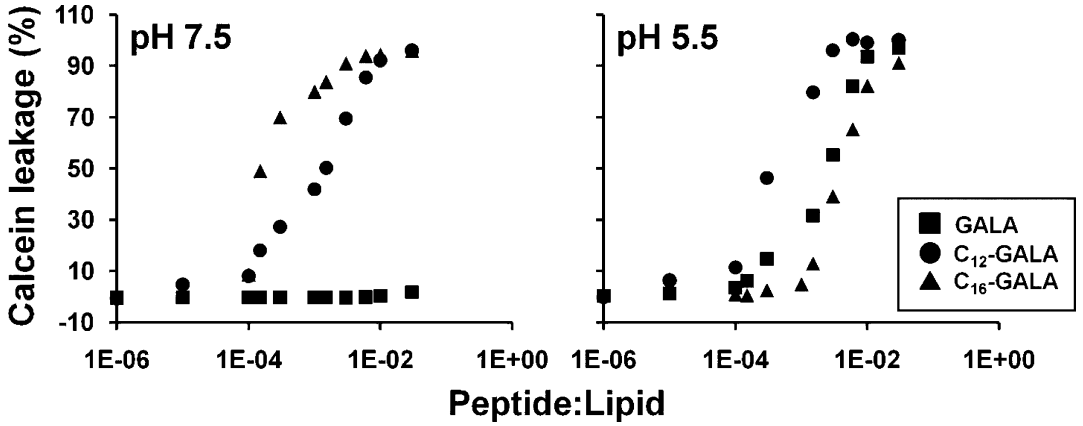

Figure 4. GALA activity is pH-dependent, while PAs induce calcein leakage independent of pH. Calcein leakage from egg PC liposomes in pH 7.5 (left) and 5.5 (right) PB/KCl buffers was recorded 2 h after the addition of GALA, C_{12}-GALA, or C_{16}-GALA.

membranes during the fixation step. Taken together, the results demonstrate that modification of GALA peptide with a lauryl tail was well tolerated by cells and furthermore increased its uptake.

DISCUSSION

Fatty acid conjugation of GALA resulted in significant changes in the physicochemical properties of the peptide and its interactions with a model bilayer membrane. GALA PAs were capable of self-assembling into micelles above a CMC, which was in the low micromolar range. Peptides in the assemblies were predominantly helical over the entire pH range studied. This observation complements a number of previous studies to the effect that acyl modification and subsequent assembly leads to enhanced peptide folding.[28−32] Induction of folding into a more native conformation has been linked to higher activity.[32,41] Since a high degree of GALA PA folding at physiological pH was a direct consequence of self-assembly, correlations between the micelle stabilized helices and their activity could not be examined. In other words, secondary structures stabilized via micellization are accessible only in the headgroup of the micelles. Since GALA and similar antimicrobial peptides are functional as monomers or in smaller assemblies, secondary structure enhancements through micellization provide no direct advantages; instead, the aggregation could potentially impede activity.[24,33]

GALA PAs disrupted liposomes through a mechanism distinct from that of GALA peptides. At physiological pH, the PAs acted on liposomes through a surfactant-like mechanism, causing membrane rupture and immediate release of encapsulated contents. In contrast, at physiological pH the peptide was inactive. At pH 5.5, both GALA peptides and PAs were able to induce the leakage of calcein while maintaining the integrity of the liposomes. For example, a 10 min incubation with C_{12}-GALA at a 1:100 P:L ratio revealed that more than 80% of calcein was released from liposomes while dextran release was not observed and liposome integrity at this time point was verified by DLS and cryo-TEM. This size-selective release of materials indicated that C_{12}-GALA was capable of forming small pores in the liposomes. However, it is not clear whether the nature of the pores was identical to the ones formed by unmodified GALA, since liposome deterioration was evident with prolonged exposure to the PA.

The hydrophobic tails of the PAs were presumed to enhance their affinity for lipid membranes.[42] As a result, PAs would partition toward membranes, which would effectively raise their local concentration and consequently reduce the overall solution concentration required for function. This trend was observed at physiological pH, where there was a direct correlation between fatty acid length and membrane disruptive potency. As predicted at pH 5.5, C_{12}-GALA exhibited higher potency as compared to GALA. Following this trend, we expected C_{16}-GALA to exhibit the highest potency; however, it appeared that its activity was more similar to that of the unmodified peptide. The possibility that micellization of C_{16}-GALA was interfering with its activity was ruled out by performing leakage experiments at lower liposome and thus peptide concentrations. One possible explanation for the lowered activity of C_{16}-GALA as compared to its lauryl counterpart could be that the palmitoyl tail interfered with the ability of PAs to form pores. Details to elucidate this mechanism will be a topic of future investigations. The membrane disruptive trend at pH 5.5 differs from that at physiological pH because the PAs disrupted lipids through a surfactant-like mechanism independent of pore formation.

Despite the finding that fatty acid attachment on GALA conferred the PAs with lytic properties, no deleterious effects on cells were observed due to nonspecific plasma membrane lysis. For the *in vitro* cell studies, the ratio of PAs to plasma membrane lipids was much higher than the theoretical value required to damage liposomes. The absence of cytotoxicity could be a result of PAs buffered by serum proteins,[43,44] which would effectively lower their toxicity. In addition, PAs bound to cells were subsequently endocytosed, which would prevent their accumulation on the plasma membrane.[39,40] Finally, differences between the egg PC liposome model and natural biological membranes, such as composition or surface curvature, could enhance the tolerance of the cells to the PAs.[21,45]

The enhanced association of PAs with liposomes translated directly to their interactions with cells, as demonstrated by the enhanced internalization of PAs over the peptide by SJSA-1 cells. Although the mechanisms of internalization are not clear at present, the punctate fluorescence pattern suggests that the peptides and PAs were located in endosomes. Whether pore formation occurred in the membrane of the endosomes is still unknown and will be the subject of our future studies. It is important to note that cell fixation dramatically altered the distribution of the peptides and PAs. Similar fixation artifacts

dx.doi.org/10.1021/bi300314h | *Biochemistry* 2012, 51, 4658−4668

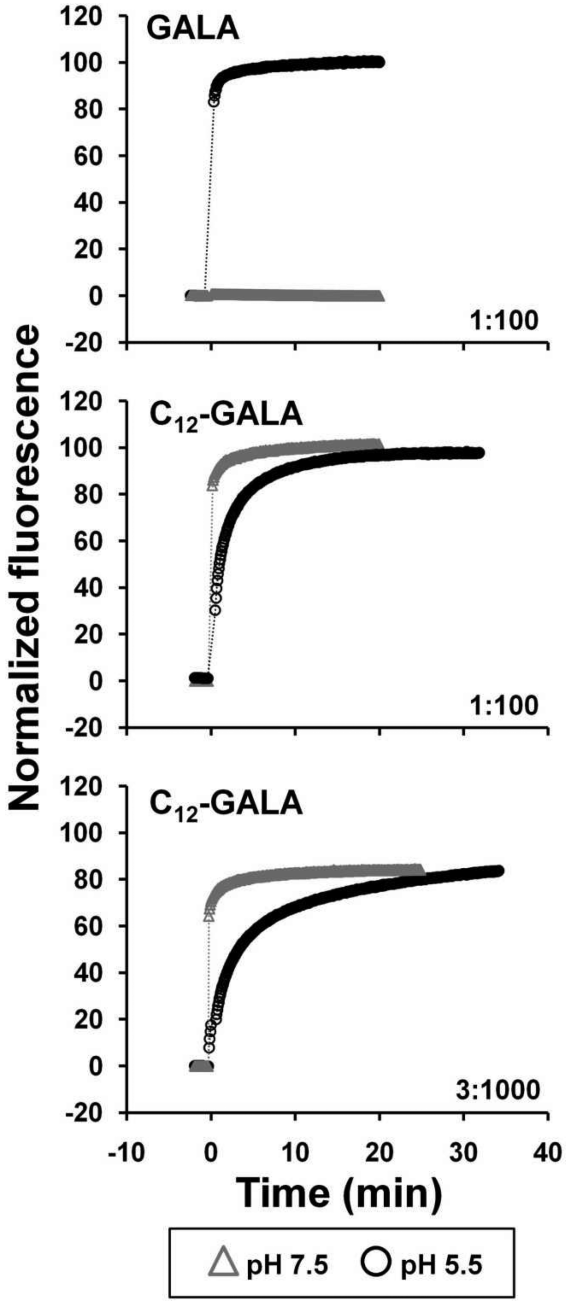

Figure 5. Calcein leakage kinetics showed that the activity of C_{12}-GALA is pH dependent. Calcein leakage from egg PC liposomes was measured every 5 s following the addition of GALA at a P:L ratio of 1:100 and C_{12}-GALA at P:L ratios of 1:100 and 3:1000, at pH 7.5 and 5.5.

Table 3. Hydrodynamic Diameter (in nm) of Egg PC Liposomes Determined by DLS, before and 30 min after Addition of GALA or C_{12}-GALA at Two Different Peptide-to-Lipid Ratios and at Two Different pH Values

	P:L ratio	pH 5.5	pH 7.5
no peptide/PA	0	159	156
GALA	1:100	170	163
	1:10	189	155
C_{12}-GALA	1:100	159	
	1:10	200	

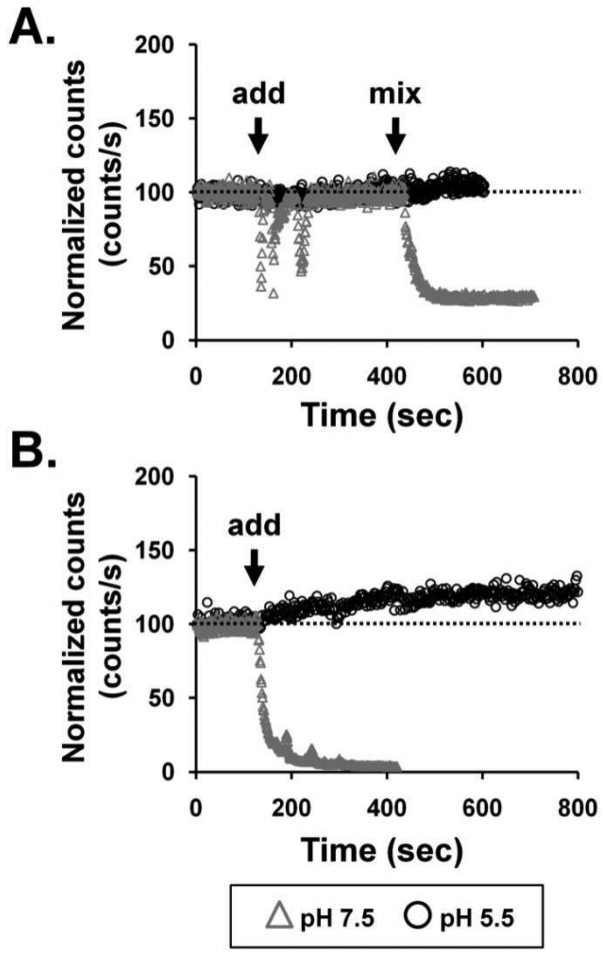

Figure 6. Short exposures of C_{12}-GALA ruptured liposomes at pH 7.5 but not at 5.5. Presented are normalized scattering intensities of 100 μM egg PC liposome suspensions as a function of time, with the addition of C_{12}-GALA at P:L ratios of 1:100 (A) and 1:10 (B). The arrows in (A) denote the addition of C_{12}-GALA and thorough mixing via pipetting. PAs was added but not mixed in (B).

were observed with cell-penetrating peptides[46] and should be kept in mind when studying peptide−cell interactions.

Finally, we consider how our results relate to the ongoing efforts for utilizing GALA peptides as part of a drug delivery system. While fatty acid modifications of GALA have been proven useful for enhancing cell interactions *in vitro*, our data in association with previously published work suggest that substituting single tails with more hydrophobic moieties might be advantageous.[14] Incorporation of C_{12}-GALA and C_{16}-GALA in liposomes is not feasible due to their lytic activity and single-tail PA micelles generally suffer from rapid breakup upon dilution or mixing with albumin.[47] In contrast, double-tail PAs have been successfully employed in micelles, which were stable enough to achieve *in vivo* targeting.[48] Moreover, doubling the number of acyl tails, to resemble natural lipids, could potentially facilitate the incorporation of PAs into liposome while avoiding their unintended lysis.[49]

In summary, we have shown that when GALA peptide is acylated, hydrophobic interactions promote self-assembly and folding irrespective over the pH range studied. The fatty acid modifications additionally altered the way the peptide interacts with model lipid bilayers. Unmodified GALA responds to acidic pH by folding into α-helices and then binding lipid membranes

dx.doi.org/10.1021/bi300314h | *Biochemistry* 2012, 51, 4658−4668

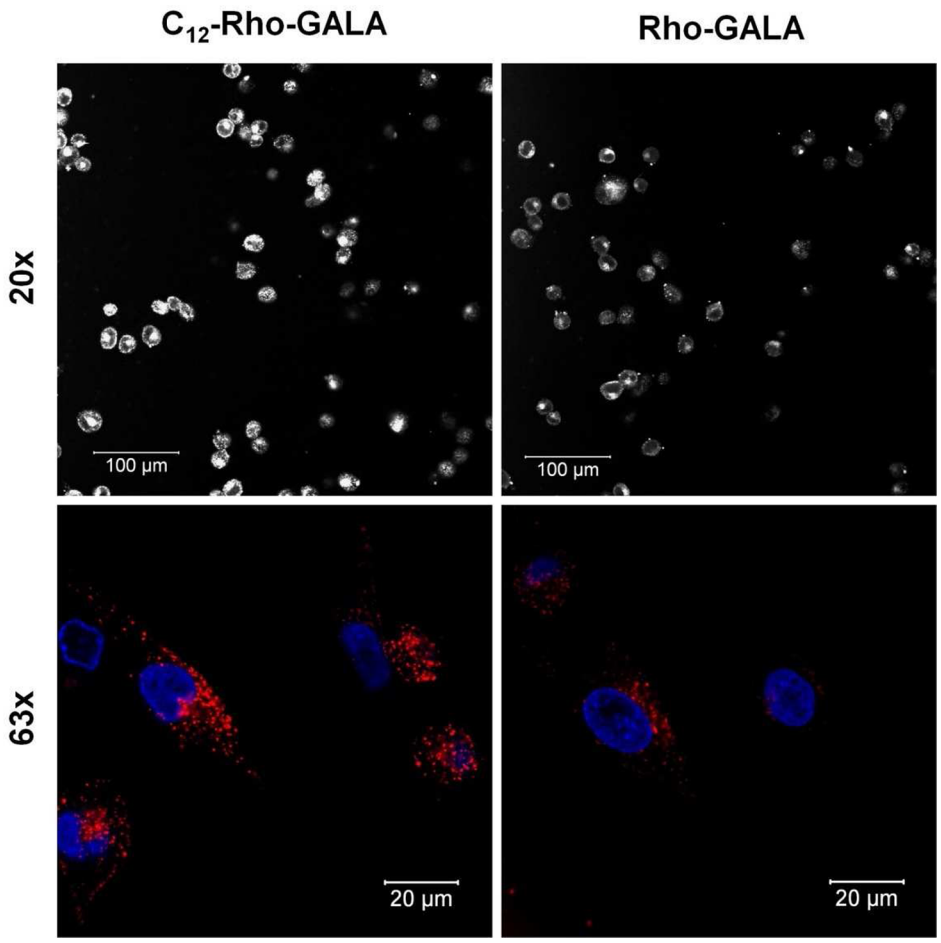

Figure 7. Rho-GALA and C_{12}-Rho-GALA internalized by SJSA-1 cells. Rho-GALA and C_{12}-Rho-GALA were incubated for 1 h with SJSA-1 cells in supplemented cell culture medium at 37 °C. Cells were then washed and live imaged using laser scanning confocal microscopy. Top row: images obtained using identical microscope settings in order to compare uptake at 20× magnification. Bottom row: higher magnification images (63×) of Rho-GALA and C_{12}-Rho-GALA (red) internalized by SJSA-1 cells. Settings were optimized, and therefore intensities cannot be directly compared. Nuclei were stained using Hoechst 33342 (blue).

and cooperatively forming transmembrane pores. PAs instead compromised the integrity of liposomes via a surfactant-like mechanism, where contents were released independently of size. The kinetics of this process was pH dependent. At pH 5.5, PAs interacted with liposomes through a mode of action, which resembled that of the peptide by forming transmembrane pores of limited size while maintaining liposome integrity. Nevertheless, prolonged exposure with PAs even at acidic pH destabilized liposomes. Despite the detrimental impact these PAs have on liposomes, *in vitro* studies showed no signs of cell toxicity and PAs exhibited enhanced cell internalization as compared to peptides. Our results provide useful insight onto the ongoing efforts and design considerations of modifying bioactive peptides with hydrophobic moieties for the development of efficient therapeutic delivery systems.

■ ASSOCIATED CONTENT

Supporting Information

Peptide/PA chemical structures (Figure S1), PA CMC measurements (Figure S2), C_{16}-GALA calcein leakage (Figure S3), dextran leakage results (Figure S4), cryo-TEM results (Figure S5), SJSA-1 MTT cytotoxicity assay (Figure S6), and confocal images of peptide/PA uptake by SJSA-1 cells after fixation (Figure S7). This material is available free of charge via the Internet at http://pubs.acs.org.

■ AUTHOR INFORMATION

Corresponding Author

*Tel +49 6221 54 4969; e-mail missirlis@uni-heidelberg.de.

Author Contributions

§Equally contributing authors.

Funding

This work was supported by National Heart, Lung and Blood Institute grant 5 U54 CA119335-04 and the MRSEC Program of the National Science Foundation under award DMR05-20415.

Notes

The authors declare no competing financial interest.

■ ACKNOWLEDGMENTS

We thank Dr. Nicolas Laugel for useful discussions and suggestions.

■ ABBREVIATIONS

CD, circular dichroism; CMC, critical micelle concentration; DLS, dynamic light scattering; FITC, fluorescein isothiocyanate; HPLC, high pressure liquid chromatography; MTT, 3-

(4,5-dimethylthiazol-2-yl)-2,5-diphenyltetrazolium) bromide; MW, molecular weight; P:L, peptide-to-lipid; PA(s), peptide amphiphile(s); PC, phosphatidylcholine; PB, phosphate buffer; PB/KCl, phosphate buffer containing potassium chloride; PBS, phosphate buffer saline; TFA, trifluoroacetic acid.

REFERENCES

(1) Wagner, E. (1999) Application of membrane-active peptides for nonviral gene delivery. *Adv. Drug Deliver Rev. 38*, 279−289.

(2) Tossi, A., Sandri, L., and Giangaspero, A. (2000) Amphipathic, alpha-helical antimicrobial peptides. *Biopolymers 55*, 4−30.

(3) Sato, H., and Felix, J. B. (2006) Peptide-membrane interactions and mechanisms of membrane destruction by amphipathic alpha-helical antimicrobial peptides. *Biochim. Biophys. Acta, Biomembr. 1758*, 1245−1256.

(4) Mastrobattista, E., van der Aa, M. A. E. M., Hennink, W. E., and Crommelin, D. J. A. (2006) Artificial viruses: a nanotechnological approach to gene delivery. *Nat. Rev. Drug Discovery 5*, 115−121.

(5) Giuliani, A., Pirri, G., Bozzi, A., Di Giulio, A., Aschi, M., and Rinaldi, A. C. (2008) Antimicrobial peptides: natural templates for synthetic membrane-active compounds. *Cell. Mol. Life Sci. 65*, 2450−2460.

(6) Chongsiriwatana, N. P., Patch, J. A., Czyzewski, A. M., Dohm, M. T., Ivankin, A., Gidalevitz, D., Zuckermann, R. N., and Barron, A. E. (2008) Peptoids that mimic the structure, function, and mechanism of helical antimicrobial peptides. *Proc. Natl. Acad. Sci. U. S. A. 105*, 2794−2799.

(7) Tossi, A., Tarantino, C., and Romeo, D. (1997) Design of synthetic antimicrobial peptides based on sequence analogy and amphipathicity. *Eur. J. Biochem. 250*, 549−558.

(8) Li, W. J., Nicol, F., and Szoka, F. C. (2004) GALA: a designed synthetic pH-responsive amphipathic peptide with applications in drug and gene delivery. *Adv. Drug Delivery Rev. 56*, 967−985.

(9) Subbarao, N. K., Parente, R. A., Szoka, F. C., Nadasdi, L., and Pongracz, K. (1987) Ph-Dependent Bilayer Destabilization by an Amphipathic Peptide. *Biochemistry 26*, 2964−2972.

(10) Parente, R. A., Nir, S., and Szoka, F. C. (1990) Mechanism of Leakage of Phospholipid Vesicle Contents Induced by the Peptide Gala. *Biochemistry 29*, 8720−8728.

(11) Haensler, J., and Szoka, F. C. (1993) Polyamidoamine Cascade Polymers Mediate Efficient Transfection of Cells in Culture. *Bioconjugate Chem. 4*, 372−379.

(12) Plank, C., Oberhauser, B., Mechtler, K., Koch, C., and Wagner, E. (1994) The Influence of Endosome-Disruptive Peptides on Gene-Transfer Using Synthetic Virus-Like Gene-Transfer Systems. *J. Biol. Chem. 269*, 12918−12924.

(13) Simoes, S., Slepushkin, V., Gaspar, R., de Lima, M. C. P., and Duzgunes, N. (1998) Gene delivery by negatively charged ternary complexes of DNA, cationic liposomes and transferrin or fusigenic peptides. *Gene Ther. 5*, 955−964.

(14) Kakudo, T., Chaki, S., Futaki, S., Nakase, I., Akaji, K., Kawakami, T., Maruyama, K., Kamiya, H., and Harashima, H. (2004) Transferrin-modified liposomes equipped with a pH-sensitive fusogenic peptide: An artificial viral-like delivery system. *Biochemistry 43*, 5618−5628.

(15) Kobayashi, S., Nakase, I., Kawabata, N., Yu, H. H., Pujals, S., Imanishi, M., Giralt, E., and Futaki, S. (2009) Cytosolic Targeting of Macromolecules Using a pH-Dependent Fusogenic Peptide in Combination with Cationic Liposomes. *Bioconjugate Chem. 20*, 953−959.

(16) Kokkoli, E., Mardilovich, A., Wedekind, A., Rexeisen, E. L., Garg, A., and Craig, J. A. (2006) Self-assembly and applications of biomimetic and bioactive peptide-amphiphiles. *Soft Matter 2*, 1015−1024.

(17) Trent, A., Marullo, R., Lin, B., Black, M., and Tirrell, M. (2011) Structural properties of soluble peptide amphiphile micelles. *Soft Matter 7*, 9572−9582.

(18) Ruoslahti, E., Bhatia, S. N., and Sailor, M. J. (2010) Targeting of drugs and nanoparticles to tumors. *J. Cell Biol. 188*, 759−768.

(19) Akita, H., Kogure, K., Moriguchi, R., Nakamura, Y., Higashi, T., Nakamura, T., Serada, S., Fujimoto, M., Naka, T., Futaki, S., and Harashima, H. (2010) Nanoparticles for ex vivo siRNA delivery to dendritic cells for cancer vaccines: Programmed endosomal escape and dissociation. *J. Controlled Release 143*, 311−317.

(20) Sasaki, K., Kogure, K., Chaki, S., Nakamura, Y., Moriguchi, R., Hamada, H., Danev, R., Nagayama, K., Futaki, S., and Harashima, H. (2008) An artificial virus-like nano carrier system: enhanced endosomal escape of nanoparticles via synergistic action of pH-sensitive fusogenic peptide derivatives. *Anal. Bioanal. Chem. 391*, 2717−2727.

(21) Puyal, C., Maurin, L., Miquel, G., Bienvenue, A., and Philippot, J. (1994) Design of a Short Membrane-Destabilizing Peptide Covalently Bound to Liposomes. *Biochim. Biophys. Acta, Biomembr. 1195*, 259−266.

(22) Cavalli, S., Albericio, F., and Kros, A. (2010) Amphiphilic peptides and their cross-disciplinary role as building blocks for nanoscience. *Chem. Soc. Rev. 39*, 241−263.

(23) Versluis, F., Marsden, H. R., and Kros, A. (2010) Power struggles in peptide-amphiphile nanostructures. *Chem. Soc. Rev. 39*, 3434−3444.

(24) Chu-Kung, A. F., Nguyen, R., Bozzelli, K. N., and Tirrell, M. (2010) Chain length dependence of antimicrobial peptide-fatty acid conjugate activity. *J. Colloid Interface Sci. 345*, 160−167.

(25) Avrahami, D., and Shai, Y. (2004) A new group of antifungal and antibacterial lipopeptides derived from non-membrane active peptides conjugated to palmitic acid. *J. Biol. Chem. 279*, 12277−12285.

(26) Lockwood, N. A., Haseman, J. R., Tirrell, M. V., and Mayo, K. H. (2004) Acylation of SC4 dodecapeptide increases bactericidal potency against Gram-positive bacteria, including drug-resistant strains. *Biochem. J. 378*, 93−103.

(27) Missirlis, D., Farine, M., Kastantin, M., Ananthanarayanan, B., Neumann, T., and Tirrell, M. (2010) Linker Chemistry Determines Secondary Structure of p53(14−29) in Peptide Amphiphile Micelles. *Bioconjugate Chem. 21*, 465−475.

(28) Yu, Y. C., Berndt, P., Tirrell, M., and Fields, G. B. (1996) Self-assembling amphiphiles for construction of protein molecular architecture. *J. Am. Chem. Soc. 118*, 12515−12520.

(29) Avrahami, D., and Shai, Y. (2002) Conjugation of a magainin analogue with lipophilic acids controls hydrophobicity, solution assembly, and cell selectivity. *Biochemistry 41*, 2254−2263.

(30) Forns, P., Lauer-Fields, J. L., Gao, S., and Fields, G. B. (2000) Induction of protein-like molecular architecture by monoalkyl hydrocarbon chains. *Biopolymers 54*, 531−546.

(31) Tu, R. S., Marullo, R., Pynn, R., Bitton, R., Bianco-Peled, H., and Tirrell, M. V. (2010) Cooperative DNA binding and assembly by a bZip peptide-amphiphile. *Soft Matter 6*, 1035−1044.

(32) Chu-Kung, A. F., Bozzelli, K. N., Lockwood, N. A., Haseman, J. R., Mayo, K. H., and Tirrell, M. V. (2004) Promotion of peptide antimicrobial activity by fatty acid conjugation. *Bioconjugate Chem. 15*, 530−535.

(33) Makovitzki, A., Avrahami, D., and Shai, Y. (2006) Ultrashort antibacterial and antifungal lipopeptides. *Proc. Natl. Acad. Sci. U. S. A. 103*, 15997−16002.

(34) Berndt, P., Fields, G. B., and Tirrell, M. (1995) Synthetic Lipidation of Peptides and Amino-Acids - Monolayer Structure and Properties. *J. Am. Chem. Soc. 117*, 9515−9522.

(35) Stroumpoulis, D., Zhang, H. N., Rubalcava, L., Gliem, J., and Tirrell, M. (2007) Cell adhesion and growth to peptide-patterned supported lipid membranes. *Langmuir 23*, 3849−3856.

(36) Stewart, J. C. M. (1980) Colorimetric Determination of Phospholipids with Ammonium Ferrothiocyanate. *Anal. Biochem. 104*, 10−14.

(37) Kalyanasundaram, K., and Thomas, J. K. (1977) Environmental Effects on Vibronic Band Intensities in Pyrene Monomer Fluorescence and Their Application in Studies of Micellar Systems. *J. Am. Chem. Soc. 99*, 2039−2044.

(38) Kuehne, J., and Murphy, R. M. (2001) Synthesis and characterization of membrane-active GALA-OKT9 conjugates. *Bioconjugate Chem. 12*, 742−749.
(39) Missirlis, D., Khant, H., and Tirrell, M. (2009) Mechanisms of Peptide Amphiphile Internalization by SJSA-1 Cells in Vitro. *Biochemistry 48*, 3304−3314.
(40) Nelson, A. R., Borland, L., Allbritton, N. L., and Sims, C. E. (2007) Myristoyl-based transport of peptides into living cell. *Biochemistry 46*, 14771−14781.
(41) Bernal, F., Tyler, A. F., Korsmeyer, S. J., Walensky, L. D., and Verdine, G. L. (2007) Reactivation of the p53 tumor suppressor pathway by a stapled p53 peptide. *J. Am. Chem. Soc. 129*, 2456−2457.
(42) Epand, R. M. (1997) Biophysical studies of lipopeptide-membrane interactions. *Biopolymers 43*, 15−24.
(43) Bhattacharya, A. A., Grune, T., and Curry, S. (2000) Crystallographic analysis reveals common modes of binding of medium and long-chain fatty acids to human serum albumin. *J. Mol. Biol. 303*, 721−732.
(44) Petitpas, I., Grune, T., Bhattacharya, A. A., and Curry, S. (2001) Crystal structures of human serum albumin complexed with monounsaturated and polyunsaturated fatty acids. *J. Mol. Biol. 314*, 955−960.
(45) Nicol, F., Nir, S., and Szoka, F. C. (1996) Effect of cholesterol and charge on pore formation in bilayer vesicles by a pH-sensitive peptide. *Biophys. J. 71*, 3288−3301.
(46) Richard, J. P., Melikov, K., Vives, E., Ramos, C., Verbeure, B., Gait, M. J., Chernomordik, L. V., and Lebleu, B. (2003) Cell-penetrating peptides - A reevaluation of the mechanism of cellular uptake. *J. Biol. Chem. 278*, 585−590.
(47) Missirlis, D., Krogstad, D. V., and Tirrell, M. (2010) Internalization of p53(14−29) Peptide Amphiphiles and Subsequent Endosomal Disruption Results in SJSA-1 Cell Death. *Mol. Pharmaceutics 7*, 2173−2184.
(48) Peters, D., Kastantin, M., Kotamraju, V. R., Karmali, P. P., Gujraty, K., Tirrell, M., and Ruoslahti, E. (2009) Targeting atherosclerosis by using modular, multifunctional micelles. *Proc. Natl. Acad. Sci. U. S. A. 106*, 9815−9819.
(49) Torchilin, V. P. (2005) Recent advances with liposomes as pharmaceutical carriers. *Nat. Rev. Drug Discovery 4*, 145−160.